Applied Physics Letters

Measurements of the femtosecond relaxation dynamics of Tamm plasmon-polaritons

Cite as: Appl. Phys. Lett. **109**, 171107 (2016); https://doi.org/10.1063/1.4966288
Submitted: 30 April 2016 • Accepted: 16 October 2016 • Published Online: 27 October 2016

B. I. Afinogenov, A. A. Popkova, V. O. Bessonov, et al.

Measurements of the femtosecond relaxation dynamics of Tamm plasmon-polaritons

B. I. Afinogenov, A. A. Popkova, V. O. Bessonov, and A. A. Fedyanin[a)]
Faculty of Physics, Lomonosov Moscow State University, Moscow 119991, Russia

(Received 30 April 2016; accepted 16 October 2016; published online 27 October 2016)

This paper reports on measurements of the lifetime of Tamm plasmon-polaritons (TPPs) excited in a 1D photonic-crystal/thin-metal-film structure. A femtosecond pulse reflected from a structure of this kind is found to be significantly distorted if its spectrum overlaps with the Tamm plasmon resonance. It is shown that the TPP lifetime possesses strong polarization and angular dependence. It varies from 20 fs for *p*-polarized light to 40 fs for *s*-polarized light at a 45° angle of incidence. The reported lifetime of Tamm plasmons is several times smaller than the previously reported lifetime of surface plasmons. *Published by AIP Publishing.* [http://dx.doi.org/10.1063/1.4966288]

In the last decade, the Tamm plasmon-polaritons (TPPs) aroused considerable interest owing to the peculiarities of their optical. TPPs are optical surface states that form at the boundary between a distributed Bragg reflector (DBR) and a metal film.[1,2] As in the case with surface plasmon-polaritons (SPPs) excitation, the emergence of TPPs leads to spatial localization of the electromagnetic field near the DBR/metal interface. However, unlike SPPs, TPPs exist for both *p* and *s* polarizations, and polarization splitting of the spectral position of the TPP resonance is observed.[3] TPPs can be detected experimentally by means of the narrow resonance in the reflectance or transmittance spectrum of a DBR/metal structure.[4] TPPs have been proposed to be used in several types of optical devices, such as sensors,[5,6] lasers,[7,8] and nonlinear-optical elements.[9] It has also been found that TPPs can be efficiently coupled with other localized states, such as SPPs,[10,11] microcavity modes,[12] and excitons.[13,14]

Studies of the ultrafast dynamics of localized optical states are driven by the desire to create compact, ultrafast, integrated photonic switches and modulators. Previously, the lifetime of SPPs was reported to be on the order of several hundred femtoseconds.[15,16] However, those values largely depend on the intrinsic properties of metals, supporting the SPP excitation. In contrast to SPPs, TPPs do not require the phase-matching conditions to be fulfilled for their excitation as well as any sophisticated excitation schemes. Moreover, the TPP-supporting structures can be easily fabricated and incorporated into micro- and nanosized optical circuits.[17,18] Thus, studying TPP femtosecond dynamics seems to be highly promising in both the theoretical and applied terms. Although the excitation dynamics of TPPs has already been discussed in Ref. 19, it dealt mainly with the complicated structures and presented only indirect measurements.

This paper focuses on measuring the TPP relaxation dynamics. An intensity cross-correlation scheme was used to measure the lifetime of a TPP in a one-dimensional photonic crystal (PC); then, the results were compared with the numerical calculations. The extent to which the lifetime depends on the angle of incidence and on polarization of the incident pulse was estimated experimentally and numerically applying the finite-difference time-domain (FDTD) technique.

The TPP lifetime is determined by figure of merit Q of the resonance. In the given sample, a Q-factor depends on the geometrical and material properties of the photonic-crystal/metal structure. Two major components can be specified here: the one related to the properties of the photonic crystal (PC) and the other related to those of the metal film. The contribution of the photonic crystal to the TPP Q-factor is determined by the number of PC layers and by difference in their refractive indexes, which precisely define the sharpness of the photonic bandgap. The amount of contribution of the metal film to the Q-factor is controlled by the film thickness and the relation between the real and imaginary parts of the refractive index of the metal. In terms of TPP-mode formation, the sharpness of the periodic potential determines the PC-related Q-factor, whereas the boundary bounce of the potential defines the metal-related Q-factor. Following the results achieved in Ref. 3. One can define TPP frequency from the condition $r_{PC}r_{Me} = 1$, where r are amplitude reflection coefficients of photonic crystal and metal, respectively. In the spectral range we have studied, the refractive index of metal possesses a significant imaginary part; thus. TPP eigenfrequencies ω_T are complex. Figure of merit of the Tamm plasmon mode is defined as $Q_T = \mathrm{Re}\ \omega_T/2\mathrm{Im}\ \omega_T$, whereas the lifetime can be approximately estimated as

$$\tau_T = \frac{1}{4\pi \mathrm{Im}\,\omega_T}.$$

By choosing different materials of PC layers, different numbers of layers, and different metals, one can efficiently tune the Q-factor of the TPP resonance and hence control the TPP lifetime. According to the numerical calculations, the lifetime can be varied from several femtoseconds to approximately hundred femtoseconds. For the reported experimental investigations, a sample possessing reasonably high $Q = 90$ was chosen.

Each studied sample of a TPP-supporting structure consisted of a $(SiO_2/Ta_2O_5)_7$ one-dimensional (1D) photonic crystal coated with a semitransparent 30-nm-thick metal film

a)Electronic mail: fedyanin@nanolab.phys.msu.ru

(Fig. 1). The thicknesses of the layers were chosen to excite TPP in the operating range of a Ti:sapphire laser; their values were 92 nm for the Ta_2O_5 layers and 130 nm for the SiO_2 layers. The films of the materials were deposited using the thermal evaporation technique; the quality of the deposition was controlled by a scanning electron microscope. The resultant sample had two distinct areas: an area of PC covered by metal and an area of a bare metal film. The latter was used for reference measurements. As for the radiation source, a Coherent Micra Ti:sapphire laser was used, as it provided 5-nJ pulses with a duration of 100 fs at the repetition rate of 80 MHz. The pulses were then compacted to have a duration of 50 fs at the position of sample using a pulse compressor. To perform the measurements, a conventional intensity cross-correlation scheme was used. Specifically, the radiation was split into signal and reference beams; then, the signal beam was reflected from the sample and superposed with the reference beam in a BBO crystal, using a parabolic mirror. The reference beam was passed through a delay line that was composed of a motorized stage with a 100-nm step, corresponding to a temporal resolution of less than 0.5 fs. The signal beam was mechanically chopped, and the noncollinear second harmonic signal from the BBO crystal was detected by a lock-in amplifier. The measurements were performed in the reflection configuration to avoid pulse broadening in the PC. The reflectance spectra were measured in the signal channel to control the TPP excitation in the sample. Figure 2 shows the reflectance spectra of a bare PC sample and a PC/Ag sample at a 45° angle of incidence for *s*-polarized radiation. The photonic bandgap of the PC lies between 610 nm and 870 nm, and a sharp TPP resonance is observed within it at $\lambda = 775$ nm. The width of the resonance was fitted employing a Lorentz line shape; the derived FWHM $\Delta\lambda$ was estimated to be 9 nm. The TPP lifetime τ_T was evaluated by using the relation $2\pi c\tau_T = \lambda^2/\Delta\lambda$, yielding a value of $\tau_T = 35$ fs.

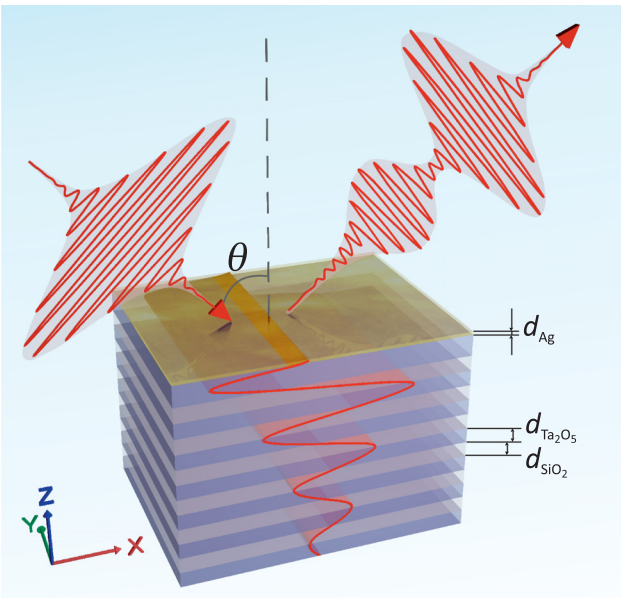

FIG. 1. Sketch of the experiment. The red curves represent incident pulse, reflected pulse and the spatial distribution of the electromagnetic field in the TPP mode: $d_{Ag} = 30$ nm, $d_{SiO_2} = 130$ nm, and $d_{Ta_2O_5} = 92$ nm.

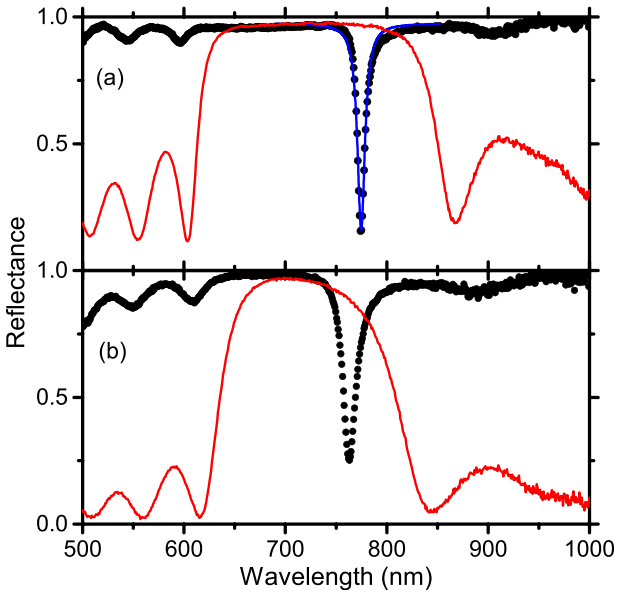

FIG. 2. Reflectance spectra of a bare photonic crystal (red dots) and a PC/Ag sample (black diamonds) measured at a 45° angle of incidence for *s*-polarized (panel a) and *p*-polarized (panel b) radiation. A Lorentzian approximation of the TPP resonance is shown by the solid curve.

A cross-correlation function (CF) of an *s*-polarized laser pulse, reflected from a PC/Ag sample at 30° angle of incidence, is shown in Fig. 3, and the corresponding spectrum is shown in inset (a). A narrow dip in the spectrum is observed around the wavelength of 800 nm, which clearly corresponds to the Tamm plasmon-polariton excitation. As soon as a pulse comes to the PC/Ag structure, energy begins to transfer to the TPP mode; shortly thereafter, it reradiates from the TPP mode to the reflected pulse. Thus, the shape of the reflected pulse results from the interference between the nonresonantly reflected part of the pulse and the component of the pulse that is being transferred into the TPP mode and

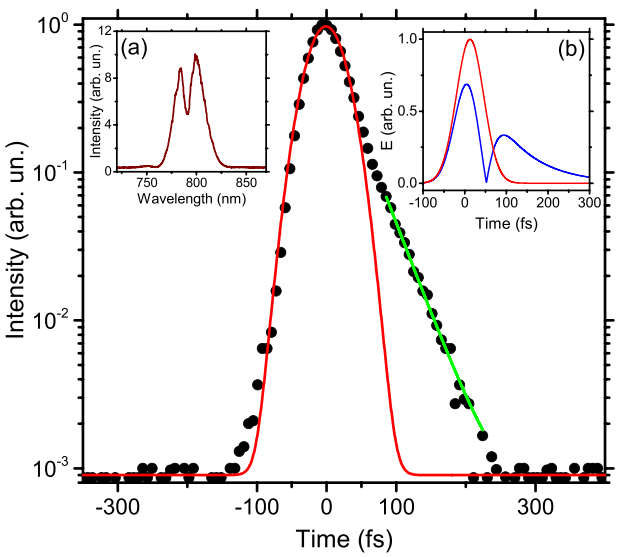

FIG. 3. Semilogarithmic plot of cross-correlation function of a *p*-polarized laser pulse reflected from photonic crystal/silver sample at 30° angle of incidence. Red curve shows an approximation with a Gaussian function, and the green line is an exponential decay fit of a trailing tail. Inset (a): Spectrum of the pulse. Inset (b): Envelopes of an incident pulse (red curve) and a reflected pulse (blue curve).

then reradiated. The corresponding cross-correlation function is being distorted and exhibits a tail on the trailing edge. This tail produced as a result of a delayed reflection of the light trapped into the Tamm plasmon mode. Decay of the intensity I of TPP mode can be comprehensively described by an exponential function $I = \exp(-t/\tau_T)$ with $\tau_T = 25$ fs, which is denoted by a green line. The signal measured in the experiment is proportional to the fourth-order field correlation function, which is given by

$$C(\tau) = \int_{-\infty}^{+\infty} E_r(t)E_r^*(t)E_s(t-\tau)E_s^*(t-\tau)dt,$$

where E_r and E_s represent the electric fields of the reference wave and the wave reflected from the sample (signal wave), respectively. The temporal profiles of the reference and signal electric fields were calculated in order to obtain the numerical cross-correlation function. By means of comparing and confronting numerical and experimental CFs, E_s was reconstructed; the result is shown in inset (b) in Figure 3 along with the envelope of the incident pulse. It is easy to notice that energy transfer process starts almost instantly after pulse hits the sample and lasts for the lifetime of the TPP mode. The exact amount of energy transferred into the Tamm plasmon depends on the amount of spectral overlapping of the TPP resonance and the spectrum of incident pulse.

As the angle of incidence increases, the light of different polarizations tends to behave differently in a photonic crystal. It can be accounted for by the fact that forming the photonic bandgap of a PC results from multipath interference in the dielectric layer stack. The reflectance of a p-polarized light decreases with an increasing angle of incidence in accordance with the Brewster's law. This leads to smoothing of the bandgap edges as well as to broadening of the TPP resonance and finally to the decrease in Q-factor. In the case with s-polarized light, the width of the TPP resonance decreases because of the increase in reflectivity at every; thus, the Q-factor increases. As the width of the resonance is related to the lifetime of a localized state, the decay rate of p-polarized Tamm plasmons goes up with an increasing angle of incidence, whereas the decay rate of s-polarized Tamm plasmons goes down. To verify the assumptions, we measured the cross-correlation functions of the p- and s-polarized laser pulses at different angles of incidence and made corresponding calculations with the help of the FDTD technique. In Figure 4, solid curves show the results of calculations; dots denote experimentally measured values, which seem to be in a reasonable agreement. The overall trend in the Tamm plasmon lifetime to a good extent corresponds to the Fresnel reflection law, as it exhibits monotonous growth for s-polarization and decline for p-polarization. Inset shows experimentally measured CFs of the pulses reflected from the PC/Ag sample at 45° angle of incidence and an autocorrelation function of the incident pulse. The CFs of reflected pulses for both the polarizations appear to be distorted as compared with the incident pulse. However, the tail of the s-polarized pulse exhibits a significantly longer decay with the time constant of 40 fs, while the corresponding lifetime of the p-polarized Tamm plasmon is 20 fs.

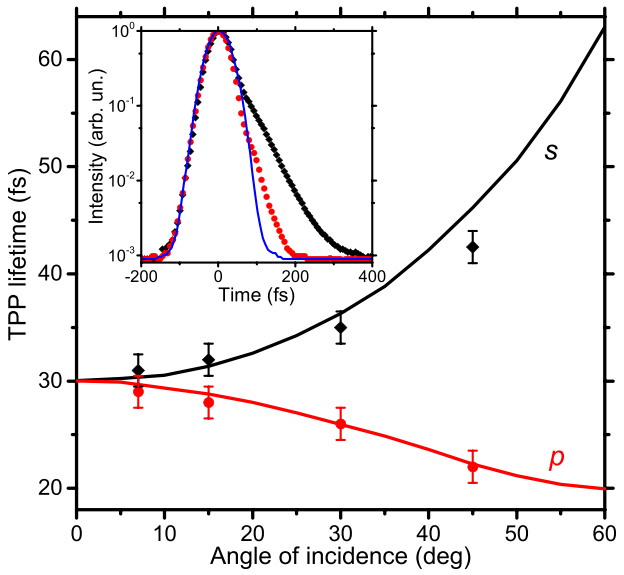

FIG. 4. Lifetime of the Tamm plasmon-polariton versus the angle of incidence for s- (black) and p- (red) polarized radiation, calculated (solid curves), and measured (dots). Inset: cross-correlation functions of laser pulses reflected from the sample at 45°. Black dots correspond to s polarization, and red dots to p polarization. Blue solid curve shows the autocorrelation function of the incident pulse.

The TPP figure of merit is affected by optical losses in metal and by the TPP mode overlapping with the metal layer.[21] In the case with the given PC/metal configuration, the figure of merit is determined by the imaginary part of the permittivity ε''. However, for the same photonic crystal excitation, the conditions of Tamm plasmon are guided by the real part of permittivity ε'. To investigate the contribution the metal makes to the TPP lifetime, we fabricated two PC samples covered with 30-nm-thick gold and silver films, respectively. Since $\varepsilon'_{Ag} \approx \varepsilon'_{Au}$ at energies of Ti:sapphire laser, Tamm plasmon in both samples is excited at approximately the same frequency. The imaginary parts of gold and silver permittivities are related[20] by the equation $\varepsilon''_{Au} \approx 3\varepsilon''_{Ag}$; thus, it is expected that the decay rate of TPP in PC/Ag sample should be less than the one in the PC/Au sample. Solid curve in Figure 5 shows the measured cross-correlation function of the s-polarized laser pulse reflected from a bare photonic crystal at a 45° angle of incidence. Since in the case under discussion no localized state is excited and the central wavelength of the pulse remains in the photonic bandgap, the whole pulse is reflected resonantly and no distortion or broadening is observed. Going back to Figure 5, the gray dots depict CF of the pulse that was reflected from the sample covered with silver film. CF exhibits a distorted trailing edge, which decays exponentially with a time constant of 40 fs. The orange diamonds denote CF of the s-polarized laser pulse reflected at 45° from the PC covered with gold. The CF also has the exponential tail, but its decay rate is bigger due to higher losses in gold, and the lifetime is equal to only 25 fs.

To conclude, let us now highlight the main stages of the conducted research. First and foremost, the measurements of the Tamm plasmon-polariton lifetime were performed. The results demonstrated that a femtosecond pulse reflected from a PC/metal sample exhibits an exponential tail due the light coupling to the TPP mode and its subsequent reradiation.

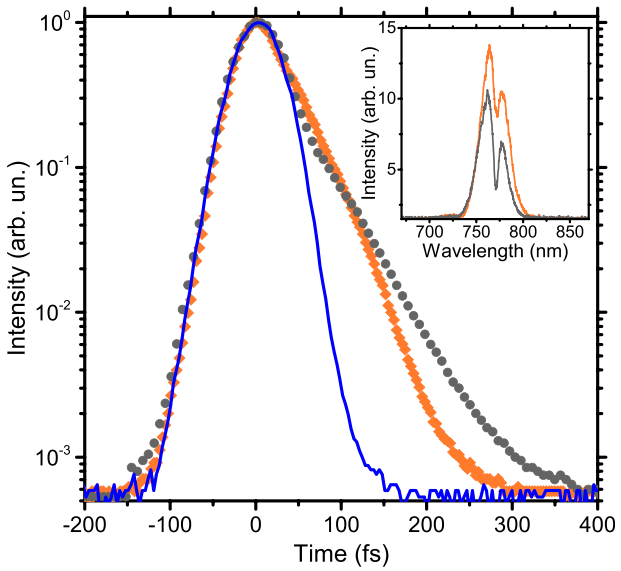

FIG. 5. Cross-correlation functions of the laser pulses reflected from a bare photonic crystal (blue curve), PC covered with gold (orange diamonds), and PC covered with silver (gray dots). Inset shows corresponding spectra.

Time, which the light needs to emit from localized state into free space, is determined by the figure of merit of photonic crystal/metal film structure and strongly depends on the angle of incidence and polarization of incoming light. Another crucial parameter that influences the lifetime of Tamm plasmons is the factor of optical losses of materials, comprising a sample. TPP decay rate strongly depends on the optical losses in metal; thus, the Tamm plasmons can be applied in the systems with fast switching of ε''. It can be realized, for instance, in the hybrid metal/graphene structures. Sharpness of corresponding resonance and short lifetime puts TPP forward as a good candidate for being used in all-optical switches and modulators.

This work was partially supported by the Russian Foundation for Basic Research (15-32-70021, 16-32-00270) (FDTD calculations) and the Russian Science Foundation (Grant No. 15-12-00065) (sample fabrication and measurements).

[1]J. A. Gaspar-Armenta and F. Villa, J. Opt. Soc. Am. B **20**, 2349 (2003).
[2]Yu. S. Kivshar, Laser Phys. Lett. **5**, 703 (2008).
[3]M. Kaliteevski, I. Iorsh, S. Brand, R. A. Abram, J. M. Chamberlain, A. V. Kavokin, and I. A. Shelykh, Phys. Rev. B **76**, 165415 (2007).
[4]A. P. Vinogradov, A. V. Dorofeenko, S. G. Erokhin, M. Inoue, A. A. Lisyansky, A. M. Merzlikin, and A. B. Granovsky, Phys. Rev. B **74**, 045128 (2006).
[5]R. Das, T. Srivastava, and R. Jha, Opt. Lett. **39**, 896 (2014).
[6]R. Badugu and J. R. Lakowicz, J. Phys. Chem. C **118**, 21558 (2014).
[7]C. Symonds, G. Lheureux, J. P. Hugonin, J. J. Greffet, J. Laverdant, G. Brucoli, A. Lemaître, P. Senellart, and J. Bellessa, Nano Lett. **13**, 3179 (2013).
[8]R. Brückner, A. A. Zakhidov, R. Scholz, M. Sudzius, S. I. Hintschich, H. Fröb, V. G. Lyssenko, and K. Leo, Nat. Photonics **6**, 322 (2012).
[9]B. I. Afinogenov, V. O. Bessonov, and A. A. Fedyanin, Opt. Lett. **39**, 6895 (2014).
[10]B. I. Afinogenov, V. O. Bessonov, A. A. Nikulin, and A. A. Fedyanin, Appl. Phys. Lett. **103**, 061112 (2013).
[11]B. Auguié, M. Cecilia Fuertes, P. C. Angelomé, N. López Abdala, G. J. A. A. Soler Illia, and A. Fainstein, ACS Photonics **1**, 775 (2014).
[12]R. Brückner, M. Sudzius, S. I. Hintschich, H. Fröb, V. G. Lyssenko, and K. Leo, Phys. Rev. B **83**, 033405 (2011).
[13]C. Symonds, A. Lemaître, E. Homeyer, J. C. Plenet, and J. Bellessa, Appl. Phys. Lett. **95**, 151114 (2009).
[14]J. Gessler, V. Baumann, M. Emmerling, M. Amthor, K. Winkler, S. Höfling, C. Schneider, and M. Kamp, Appl. Phys. Lett. **105**, 181107 (2014).
[15]C. Ropers, D. J. Park, G. Stibenz, G. Steinmeyer, J. Kim, D. S. Kim, and C. Lienau, Phys. Rev. Lett. **94**, 113901 (2005).
[16]P. P. Vabishchevich, V. O. Bessonov, F. Y. Sychev, M. R. Shcherbakov, T. V. Dolgova, and A. A. Fedyanin, JETP Lett. **92**, 575 (2010).
[17]M. Deubel, G. von Freymann, M. Wegener, S. Pereira, K. Busch, and C. M. Soukoulis, Nat. Materials **3**, 444 (2004).
[18]M. Suzuki, M. Aoki, M. Takahashi, and T. Taniwatari (Hitachi Ltd.), U.S. patent 5,543,353 (6 August 1996).
[19]P. Melentiev, A. Afanasiev, and V. Balykin, Phys. Rev. A **88**, 053841 (2013).
[20]P. B. Johnson and R. W. Christy, Phys. Rev. B **6**, 4370 (1972).
[21]M. A. Kaliteevski, A. A. Lazarenko, N. D. Ilinskaya, Yu. M. Zadiranov, M. E. Sasin, D. Zaitsev, V. A. Mazlin, P. N. Brunkov, S. I. Pavlov, and A. Yu. Egorov, Plasmonics **10**, 281 (2015).